

Buoyancy Heat Transfer In Staggered Dividing Square Enclosure

Ali L. Ekaid* , Ayad F. Hameed* & Ahmad F. Mehde**

Received on:1/4/2009

Accepted on:5/11/2009

Abstract:

In this research, the Buoyancy heat transfer and flow patterns in a partially divided square enclosure with staggered partitions have been studied numerically. The partitions were distributed on the lower and upper surfaces of the box in staggered manner. The height of the partitions was varied. The conduction heat transfer through the fins (partitions) was also included. It is assumed that the vertical walls of enclosure were adiabatic and its horizontal walls were maintained at uniform but in different temperature. The problem was formulated in terms of the stream function-vorticity procedure. The numerical solution based on the transformation of the governing equations by using finite difference method was obtained. The effect of increasing the partition height and Rayleigh number on contour maps of the stream lines and temperature were reported and discussed. In addition, the research presented and discussed the results of the average Nussult number of the enclosures heated wall at various Rayleigh number and dimensionless partition heights. The results showed that the mean Nussult number increases with the increasing of Rayleigh number and decreases with the increasing of partition heights. The distributed heat by conduction through the partition increases with the increasing of the partition height especially at ($H/L \geq 0.3$). A comparison between the obtained results and the published computational studies has been made and it showed a good agreement with percentage error not exceed (0.54%).

Keywords: CFD, Buoyancy heat transfer, staggered partitions, square enclosure.

انتقال الحرارة بالطفو داخل حيز مقسم بحواجز ذات ترتيب متخالف

الخلاصة:

تضمن البحث دراسة انتقال الحرارة بالطفو وشكل خطوط الجريان داخل حيز مربع بوجود حواجز بترتيب متخالف عددياً. وزعت الحواجز على سطحي الحيز الأسفل والأعلى بشكل متخالف، مع تغيير ارتفاع الحواجز. كما تم دراسة انتقال الحرارة بالتوصيل خلال الزعانف (الحواجز). افترضت الجدران العمودية للحيز أدبياتية والجدران الأفقية ذات درجة حرارة منتظمة لكن مختلفة. مثلت المشكلة باستخدام طريقة دالة الانسياب - الدوامية. وتم الحصول على الحل العددي عن طريق تحويل المعادلات الحاكمة باستخدام طريقة الفروق المحددة. كما درس تأثير كل من ارتفاع الحواجز ورقم رايلي على مخططات السرعة ودرجات الحرارة، بالإضافة إلى مناقشة النتائج الخاصة بمعدل عدد نسلت للجدار المسخن في الحيز لأرقام رايلي وارتفاعات الحواجز اللابعدية مختلفة. بينت النتائج أن عدد نسلت الإجمالي يزداد مع ازدياد عدد رايلي ويقل مع ازدياد ارتفاع الحواجز، الحرارة الموزعة بالتوصيل تزداد مع ازدياد ارتفاع الحواجز خاصة عند ($H/L \geq 0.3$). قورنت النتائج الحالية مع نتائج عديدة منشورة وتبين أن التوافق جيد بينهما وبنسبة خطأ لا تتجاوز (0.57%).

*Mechanical Engineering Department, University of Technology/ Baghdad

** Manufacturing Operation Department, Al- Khwarizmi Engineering College/ Baghdad

Introduction

Natural convection in an enclosure with partial vertical divider has received considerable degree of recent interest. This interest stems from the significance of buoyancy-induced flows in various engineering and technological applications such as convective heat loss from solar collectors, thermal insulation, nuclear reactors, heat-recovery systems, energy conservation in buildings, air conditioning and ventilation, cooling of electronic equipments, and semiconductor production.

Many scientists and researchers have been studied the natural heat transfer and fluid flow in square enclosure with and without divided partitions to see the effect of partitions on the heat transfer mechanism inside the space, Karayiannis et. al. [1] studied the Convective heat transfer for air in rectangular cavities without a partition and with a vertical partition with different constant temperatures on the opposite walls numerically. The aspect ratio changed from (0.1) to (16), and the Rayleigh number from (3.5E3) to (3.5E7) (for cavities without partitions) and from (1E5) to (1.6E8) (for cavities with partitions), with the partition thickness and thermal conductivity being varied, the Nusselt number reduced by (12%) due to the partition. Yucel and Ozdem [2] have studied natural convection in partially divided square enclosures. They have concluded that the mean Nusselt number

decreases with increasing the height and number of partitions. Dagtekin and Oztop [3] have investigated natural convection heat transfer by heated partitions within an enclosure. They have found that as the partitions, height increases, the mean Nusselt number increases and that the position of partitions have more effects on fluid flow than that of heat transfer. Abdullatif and Ali [4] study laminar natural convection flow of a viscous fluid in an inclined enclosure with partitions, the range of Rayleigh and the angle of inclination was (1E3 to 1E6) and (0-90o) respectively. It was found that the average Nusselt number increases with increase in the Rayleigh number. Also, as the dimensionless partition height increases, the flow speed within the partitioned enclosure decreases resulting in less wall heat transfer. In addition, the average Nusselt number was found to decrease as the partitioned enclosure inclination angle was increased beyond (30°). Nansteel and Greif [5, 6] performed experiments on natural convection heat transfer in undivided and partially divided rectangular enclosures. In their studies, the vertical walls were maintained different temperatures while the horizontal walls were adiabatic. The experiment carried out with water for Rayleigh numbers over the range (1E10–1E11). The vertical partial partition was fitted the top surface. The correlations for the average Nusselt number were generated for

the cases of conducting and non-conducting partial divisions as a function of Rayleigh number and aperture ratio (height of partition height of enclosure). The partial divisions were shown to significantly decrease the overall heat transfer, especially when the partitions were non-conducting. Lakhali et. al. [7] study numerically the natural convection in inclined rectangular enclosure with perfectly conducting fins attached to the heated wall. The parameter governing this problem are the Rayleigh (1E2-2E5), the aspect ratio (2.5- 10), and the inclination angle (0- 60°). the results indicate that the heat transfer through the cover is considerably effected by the presences of the fin. Also at low Rayleigh numbers the heat transfer regime is dominated by conduction.

In the present study, natural convection in partially staggered partitioned square enclosures is considered. The vertical walls are assumed to be adiabatic and horizontal top and bottom walls are kept at constant but different temperatures. The partitions having finite thickness and finite thermal conductivity are attached to the bottom and the top walls of the enclosure in staggered manner. A computer program is developed on the basis of the finite difference method. The fluid flow and temperature fields are predicted for different Rayleigh numbers, and partition heights. From the temperature fields predicted, the average Nusselt numbers are calculated.

The mathematical model

The physical domain considered in this study is a (2-D) square enclosure with partially divided staggered partitions which is shown in Fig. (1) The length of the side of the square is denoted by (L). The thickness and length of partitions are represented by (d and H), respectively.

Considering, steady laminar, two-dimensional, natural convective flow inside partitioned enclosure. The temperatures (Th) and (Tc) are uniformly imposed on two opposing horizontal walls such that (Th> Tc) while the other walls are assumed to be adiabatic. Fig. (1) Shows the schematic and coordinate system of the problem under consideration. The fluid is assumed to be incompressible, Newtonian and viscous and has constant thermo-physical properties except the density in the buoyancy term of the momentum equations. The effect due to viscous dissipation is assumed to be negligible.

The governing equations for this problem are based on the balance laws of mass, linear momentum and energy. Taking into account the assumptions mentioned above, and applying the Boussinesq approximation for the body force terms in the momentum equations, the governing equations can be written in dimensionless stream function-vorticity form as:

$$U \frac{\partial z}{\partial X} + V \frac{\partial z}{\partial Y} = Pr \left(\frac{\partial^2 z}{\partial X^2} + \frac{\partial^2 z}{\partial Y^2} \right) + \dots(1)$$

$$Ra Pr \frac{\partial q}{\partial X}$$

$$\frac{\partial^2 y}{\partial X^2} + \frac{\partial^2 y}{\partial Y^2} = -z \quad \dots(2)$$

$$U \frac{\partial q}{\partial X} + V \frac{\partial q}{\partial Y} = \frac{\partial^2 q}{\partial X^2} + \frac{\partial^2 q}{\partial Y^2} \quad \dots(3)$$

Where: the dimensionless stream function and vorticity are defined in the usual way as:

$$U = \frac{\partial y}{\partial Y}, \quad V = \frac{\partial y}{\partial X}, \quad z = \frac{\partial v}{\partial X} - \frac{\partial u}{\partial Y} \quad \dots(4)$$

For the solid region (in the partitions), the energy equation for the heat transfer by conduction (Eq. (3)) becomes:

$$\frac{\partial^2 q}{\partial X^2} + \frac{\partial^2 q}{\partial Y^2} = 0 \quad \dots(5)$$

The following equation was defined for the interface between the solid and fluid [8]:

$$K_f \frac{\partial q}{\partial n} = K_s \frac{\partial q}{\partial n} \quad \dots(6)$$

Where: (Kf) and (Ks) is the thermal conductivity of fluid and solid respectively, (n) represent the normal distance.

The governing equations are converted into the non-dimensional form by defining the following non-dimensional variables:

$$X = \frac{x}{L}, \quad Y = \frac{y}{L}, \quad z = \frac{wL^2}{a},$$

$$y = \frac{\Psi}{a}, \quad q = \frac{T - T_c}{T_h - T_c},$$

$$Pr = \frac{n}{a}, \quad Ra = \frac{gb(T_h - T_c)L^3}{an} \quad \dots(7)$$

The equations (1, 2, 3, 5) are subjected to the following boundary conditions:

1. the left wall (X=0) and the right wall (X=1): $\frac{\partial q}{\partial X} = 0$
2. the lower wall (Y=0): $q = 1$
3. The upper wall (Y=1): $q = 0$
4. For the all surface walls: $y = 0$
5. For the all surface walls: $(z_0 = \frac{3}{\Delta n^2}(y_0 - y_1) + \frac{1}{2}z_1)$

woods condition.

The heat transfer rate (Nussult number) was calculated along the lower surface (heated wall) according to the equation:

$$\overline{Nu} = \int_0^1 \frac{\partial q}{\partial Y} \Big|_{Y=0} dX \quad \dots(8)$$

Numerical Solution

The governing equations (1,2,3,5) are solved by finite difference scheme which used central differencing for the second order derivative and upwind or one-sided differencing for non linear first order convective terms. The role of upwind differencing procedure in stabilizing the numerical scheme has been well documented. The application of this scheme to free convection flow at high Rayleigh number is discussed in [9].

Following is the procedure in [9], the governing finite difference equations for (ζ , Θ , and ψ) can be written in the standard five point formula form. These finite difference

equations which subject to appropriate boundary conditions are solved by an iterative method known as successive substitution. If (z^s, q^s, y^s) and (q^s) denote functional values at the end of sth iteration, the value of (z, q, y) at (s+1)th iteration level are calculated from the following expressions,

$$z_{i,j}^{s+1} = (1 - g_z)z_{i,j}^s + \frac{g_z}{A_z} [a_z z_{i+1,j}^s + b_z z_{i-1,j}^{s+1} + c_z z_{i,j+1}^s + d_z z_{i,j-1}^{s+1} + 0.5 Ra Pr h(q_{i+1,j}^{s+1} - q_{i-1,j}^{s+1})]$$

$$q_{i,j}^{s+1} = (1 - g_q)q_{i,j}^s + \frac{g_q}{A_q} (a_q q_{i+1,j}^s + b_q q_{i-1,j}^{s+1} + c_q q_{i,j}^s + d_q q_{i,j-1}^{s+1})$$

$$y_{i,j}^{s+1} = (1 - g_y)y_{i,j}^{s+1} + \frac{g_y}{4} (y_{i+1,j}^s + y_{i-1,j}^{s+1} + y_{i,j+1}^s + y_{i,j-1}^{s+1} + h^2 w_{i,j}^{s+1})$$

$$q_{i,j}^{s+1} = (1 - g_{qso})q_{i,j}^{s+1} + \frac{g_{qso}}{4} (q_{i+1,j}^s + q_{i-1,j}^{s+1} + q_{i,j+1}^s + q_{i,j-1}^{s+1})$$

... (9)

Where (h) is the step size and $(\gamma_\zeta, \gamma_\theta, \gamma_\psi, \text{ and } \gamma_{\theta so})$ are over relaxation parameter which depend on the mesh size and fluid mechanical parameters and (A_ζ, A_θ) are given in [9].

For the interface region, the equation (6) is solved forward or backward according to the location of the partition. The final form of equation (6) is:

$$q_{int} = (K_r q_f + q_s) / (1 + K_r) \dots (10)$$

A converged solution was defined as one that meet the following criterion for all dependent variables.

$$|f^{n+1} - f^n| \leq 10^{-4} \dots (11)$$

Results and discussions

The heat transfer in partially divided square enclosures and the fluid flow were numerically investigated. It is assumed that the Left and the right walls of enclosures are adiabatic and the upper and the lower walls of enclosures are maintained at uniform but different temperatures. By assuming the enclosure contains air, hence (Pr) is taken to be (0.7) in the fluid region. Partitions are placed on horizontal surfaces in staggered manner, their dimensionless heights (H/L) are taken (0.0, 0.1, 0.2, 0.3, 0.4, and 0.5), and the thicknesses (d/L) are taken (0.1).

Dimensionless locations of partitions ($w_1/L, w_2/L, w_3/L, w_4/L, w_5/L, w_6/L$) are chosen as (0.15, 0.45, 0.75, 0.3, 0.6, and 0.9) respectively.

In the partition regions (k_f) is taken as (8416.66) (which represents the ratio of the thermal conductivity of aluminum to that of air). Computations are performed at different Rayleigh numbers in the range ($10^3, 10^4, 10^5, 3*10^5, 4*10^5, 5*10^5, 7*10^5, \text{ and } 10^6$), for the different dimensionless partitions heights. In order to investigate fluid structure and heat transfer, the streamline and isotherm contours are drawn and mean Nusselt number is

calculated from the local Nusselt number for each case.

Fig.(2) shows the temperature contours for different Rayleigh numbers plotted for a ($H/L=0.0$) case (no partition) with adiabatic vertical walls. As seen in Fig. (2), when the Rayleigh number increases, the temperature gradient next to hot and cold wall increases. Also development of the plume effect can be seen as the Rayleigh number increases.

In Fig. (3), the streamline contours for different Rayleigh numbers are plotted, at low Rayleigh number there are two circulating cells with opposite direction in the lower half of the enclosure, as the Rayleigh number increased the two circulating cells stretched and shifted upward, also the flow (stream function) become more strongly.

Fig.(4) shows the temperature contours for different Rayleigh numbers for ($H/L=0.1$). also when the Rayleigh number increases, the temperature gradient next to hot and cold wall increases. But the symmetry of the temperature region about the vertical mid line change duo to the presence of the partitions which develop conduction heat transfer. It can be seen that the plume temperature region shifted to the right wall duo to the staggered distribution of the partitions.

In Fig. (5), the streamline contours for ($H/L=0.1$) are plotted, the two circulating cells with opposite direction also found in the enclosure, the effect of staggered partitions clearly seen by shifting the right circulating cell to the right wall, as the Rayleigh number increased the two circulating cells stretched and

shifted upward, also the strength of the flow become more strongly.

Fig.(6) shows the temperature contours for different Rayleigh numbers for ($H/L=0.2$). The temperature distribution continuous to move toward the right vertical wall which demonstrate the effect of heat conducted from the lower partitions (especially from the second and the third partition). the left circulated cell of the streamline contour for the same value of (H/L) will growth as the Rayleigh numbers increases, that growth will squeeze the other cell. A third cell will appear at the high Rayleigh number, that is clearly appear in fig.(7).

As the height of the staggered partitions increases ($H/L=0.3, 0.4, 0.5$) Fig. (8, 10, and 12), the conduction heat transfer will dominate in the enclosure and the effect of heat transfer by convection will be less than of conduction heat transfer due to increase the height of the partitions, in other word the heat exchange by conduction between the hot partitions and the cold one is increased as they come close to each other. Also the plume effect will diminish after the ratio ($H/L > 0.3$) which illustrate the dominate of conduction heat transfer on the convection heat transfer.

For the flow inside the enclosure, increasing the height of the staggered partitions will effect the streamline contour strongly, as shown in Fig.(9, 11, and 13) the number of circulating cells will increase until almost each of the zones between the partitions will contain one cell, that is clear at ($H/L \geq 0.4$), also the gradient of stream

function will increase near the partitions wall as both Rayleigh number and the height of partitions increased.

As shown in Fig.(14), the heat transfer rate or the average Nussult number increase with increasing the Rayleigh number for each dimensionless partition height. and decrease as the dimensionless partition height increased for each Rayleigh number, as the Rayleigh number and dimensionless partition height increase ($Ra=10^3$ to 10^6) and ($H/L = 0.0$ to 0.5) respectively. The increasing in heat transfer will change from (23% to 11%).

Fig. (15) Shows the comparison between the present study and [2], as shown in Fig. the agreement is good between both studies with percentage error not exceed (0.54%).

Conclusions

1. The heat transfer increase and the plume shape of natural heat transfer appear with increasing the Rayleigh number.
2. The flow structure is strongly affected by increasing the Rayleigh number.
3. The symmetry of the heat transfer region is changed and affected by the presences of staggered partitions.
4. The flow structure is strongly affected by presences of staggered partitions especially at ($H/L \geq 0.4$).
5. The conduction heat transfer appear after ($H/L=0.3$).
6. At high (H/L), the Nussult number increased in a less

rate as Rayleigh number increased.

References

- [1]. T. G. Karayiannis, M. Ciofalo, and G. Barbaro, " On natural convection in a single and two zone rectangular enclosure" *Int. J. Heat Mass Transfer*, Vol. 35, No. 7, p.p.(1645-1657), (1992).
- [2]. Yucel N., Ozdem A.H., "Natural convection in partially divided square enclosures", *Heat and Mass Transfer*, Vol. 40, p.p.(167-175), (2003).
- [3]. Dagtekin I, Oztop H.F., "Natural convection heat transfer by heated partitions within enclosure". *Int. Journal of Heat and Mass Transfer*, Vol. 28, p.p.(823-834), (2001).
- [4]. Abdullatif B. Nakhi and Ali J. Chamkha., "Natural convection in inclined partitioned enclosures", *Heat Mass Transfer*, Vol. 42, p.p.(311-321), (2006).
- [5]. Nansteel M.W., Greif R., "Natural convection in undivided and partially divided rectangular enclosures". *Journal of Heat Transfer*, Vol. 103, p.p.(623-629), (1981).
- [6]. Nansteel M.W., Greif R., "An investigation of natural convection in enclosures with two- and three-dimensional partitions". *Int. Journal Heat Transfer*. Vol. 27, p.p.(561-571), (1984).
- [7].E. K. Lakhali, M. Hasnaoui, E. Bilgen, P. Vasseur., "Natural convection in inclined rectangular enclosures with perfectly conducting fins attached on the heated wall". *Heat and mass transfer*, Vol. 32, p.p.(365-373), (1997).

[8].I.V. Marchuk, O. A. Kabov, "Numerical simulation of heat transfer liquid film with allowance for heat conduction in heaters". *Russ. J. Eng. Thermophys.*, Vol. 10, No. 2, p.p.(147-165), (2000).

[9].E.F. Nogotov, "Applications of Numerical heat transfer", Hemisphere publishing corp. Washington. (1978).

List of Symbol

Symbol	Description	Unit
d	Thickness of the partition	m
g	Gravitational acceleration	m/sec ²
H	Height of the partition	m
K _s	Thermal conductivity of the partition (solid)	W/m.K
k _f	Thermal conductivity of fluid	W/m.K
k _r	Thermal conductivity ratio	kr = k _s /k _f
L	Length of the cavity	m
n	Normal distance	—
\overline{Nu}	Mean Nusselt number	—
Pr	Prandtl number (Pr = ν_f/α_f)	—
Ra	Rayleigh number Ra = $g\beta(T_H - T_C)L^3/\nu_f\alpha_f$	—
T	Temperature	K
T _c	Cold wall temperature	K
T _h	Hot wall temperature	K
U	Dimensionless velocity component in x-direction	—
V	Dimensionless velocity component in y-direction	—
x	Horizontal axis	m
X	Dimensionless horizontal axis (X = x/L)	—
y	Vertical axis	m
Y	Dimensionless vertical axis (Y = y/L)	—
α	Thermal diffusivity of fluid	m ² /sec
β	Thermal expansion coefficient	K ⁻¹

ν	Kinematic viscosity	m^2/sec
θ	Dimensionless temperature ($\theta = (T - T_c) / (T_h - T_c)$)	—
ψ	Stream function	—
Ψ	Dimensionless Stream function	—
ω	Vorticity	—
ζ	Dimensionless Vorticity	—

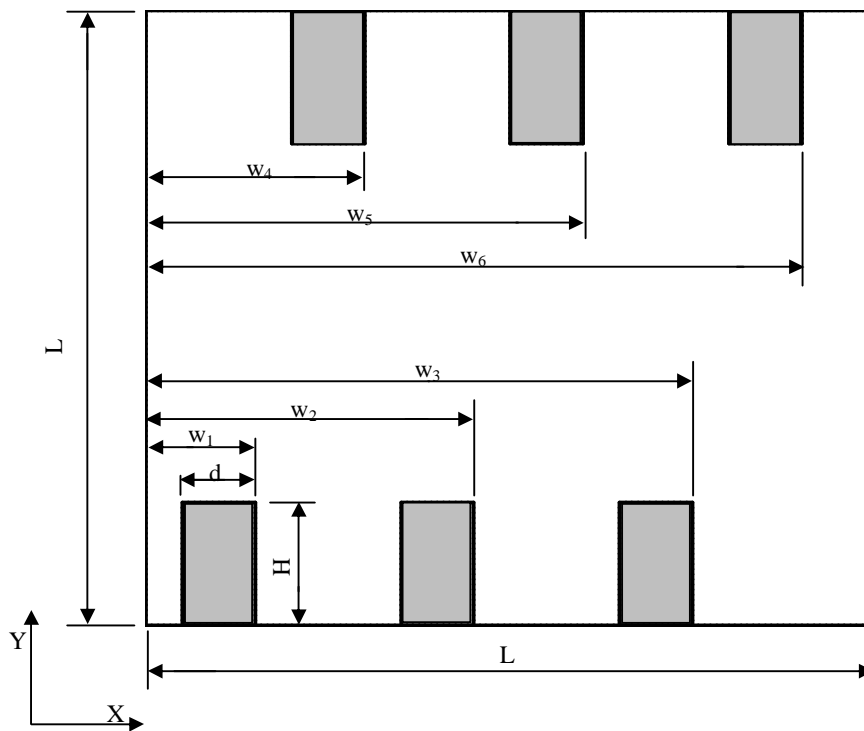


Figure (1) Problem schematic and coordinate system.

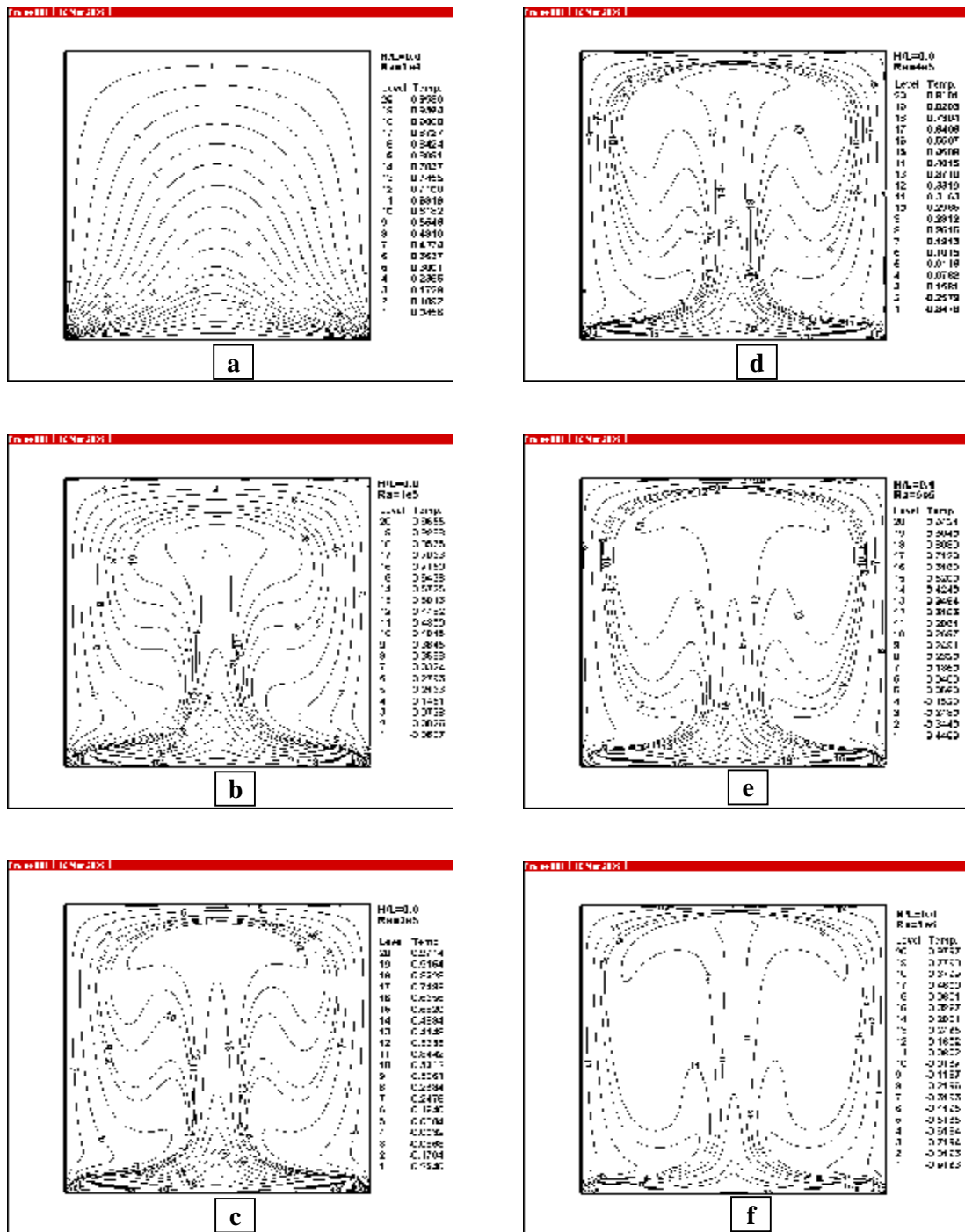


Figure (2) Temperature contours at $H/L=0.0$ with different Rayleigh Number (a. $Ra=1 \times 10^4$, b. $Ra=1 \times 10^5$, c. $Ra=3 \times 10^5$, d. $Ra=1 \times 10^4$, e. $Ra=5 \times 10^5$, and f. $Ra=1 \times 10^6$).

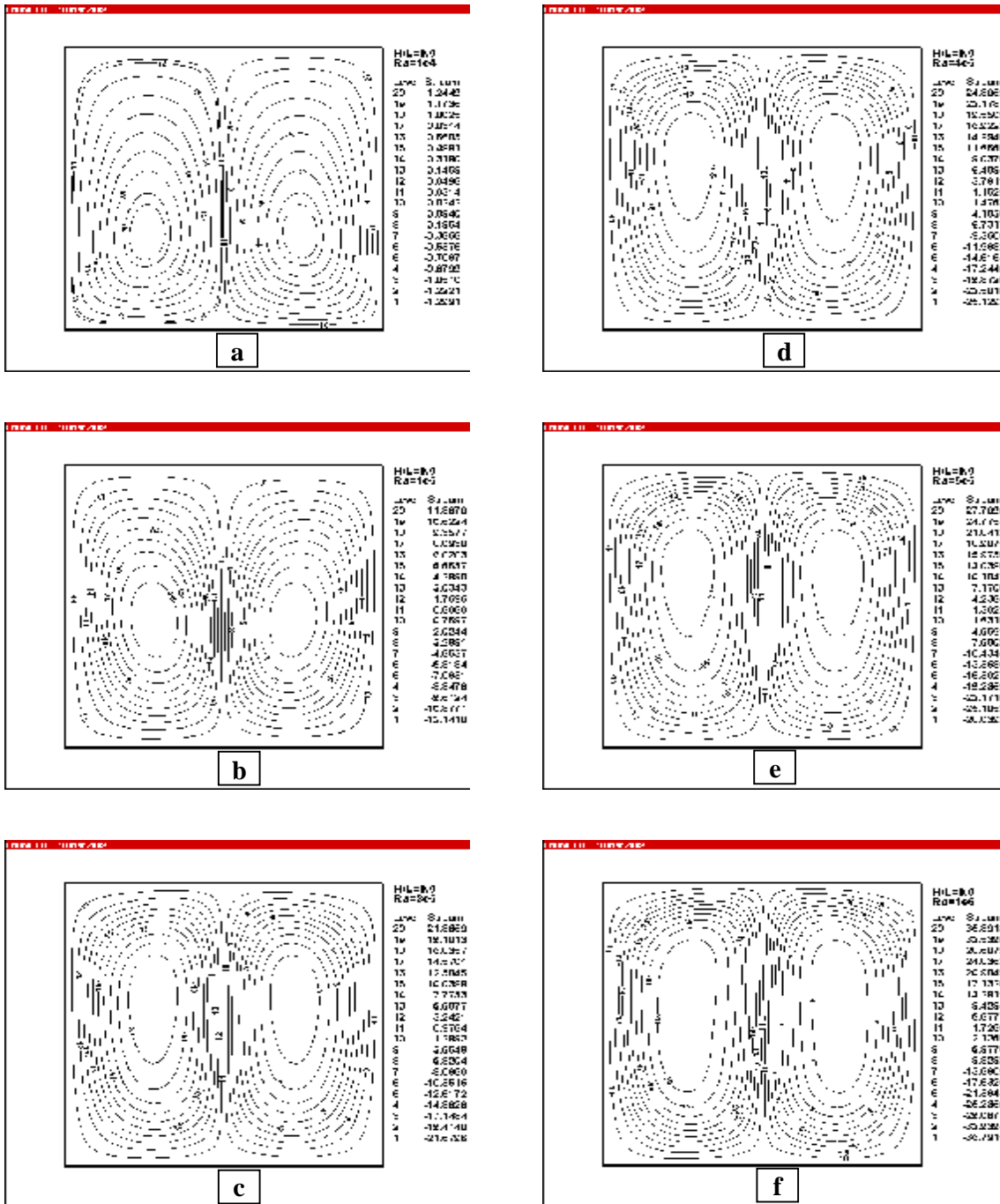


Figure (3) Stream contours at $H/L=0.0$ with different Rayleigh Number (a. $Ra=1 \times 10^4$, b. $Ra=1 \times 10^5$, c. $Ra=3 \times 10^5$, d. $Ra=1 \times 10^4$, e. $Ra=5 \times 10^5$, and f. $Ra=1 \times 10^6$).

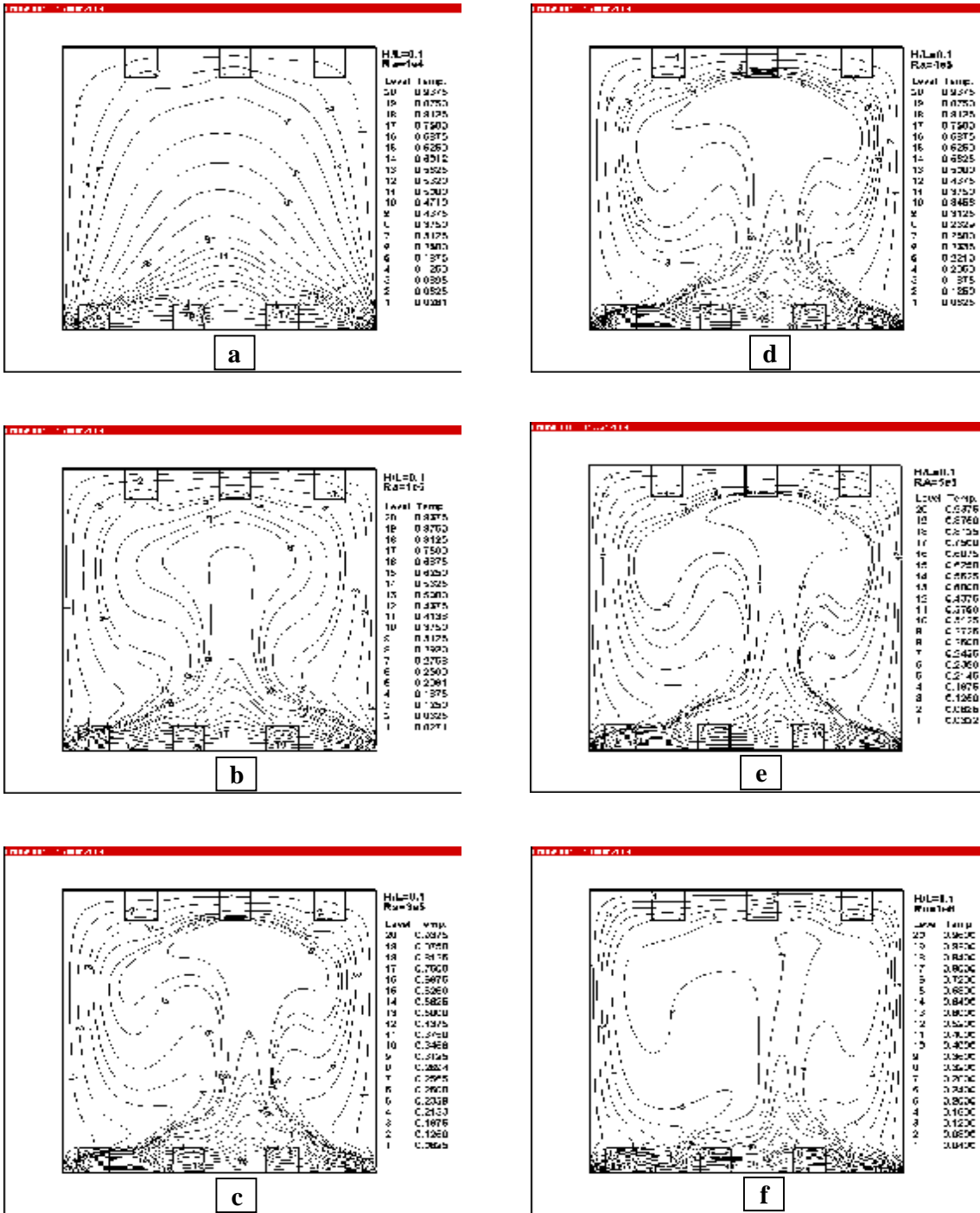


Figure (4) Temperature contours at $H/L=0.1$ with different Rayleigh Number (a. $Ra=1 \times 10^4$, b. $Ra=1 \times 10^5$, c. $Ra=3 \times 10^5$, d. $Ra=1 \times 10^4$, e. $Ra=5 \times 10^5$, and f. $Ra=1 \times 10^6$).

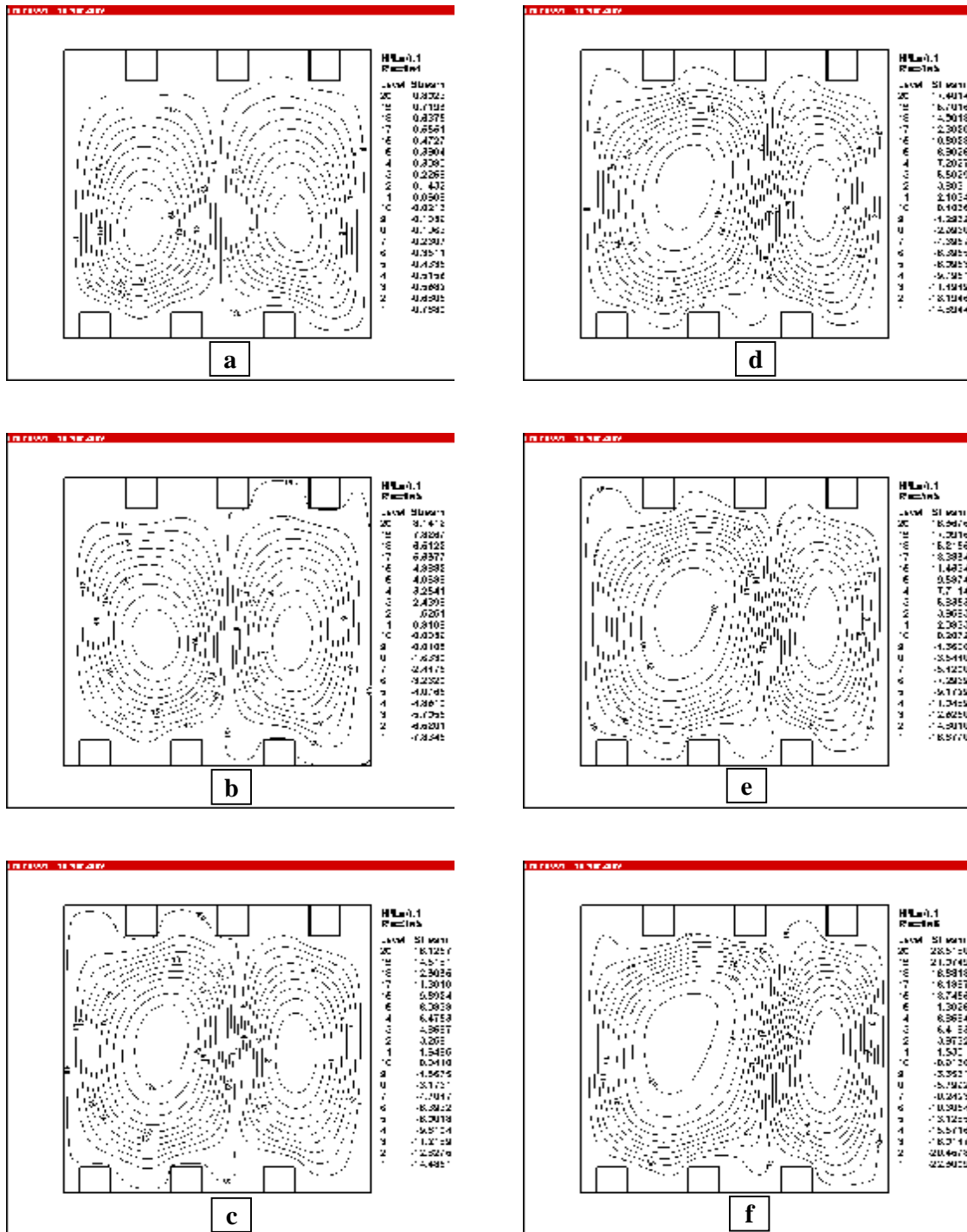


Figure (5) Stream contours at $H/L=0.1$ with different Rayleigh Number (a. $Ra=1 \times 10^4$, b. $Ra=1 \times 10^5$, c. $Ra=3 \times 10^5$, d. $Ra=1 \times 10^4$, e. $Ra=5 \times 10^5$, and f. $Ra=1 \times 10^6$).

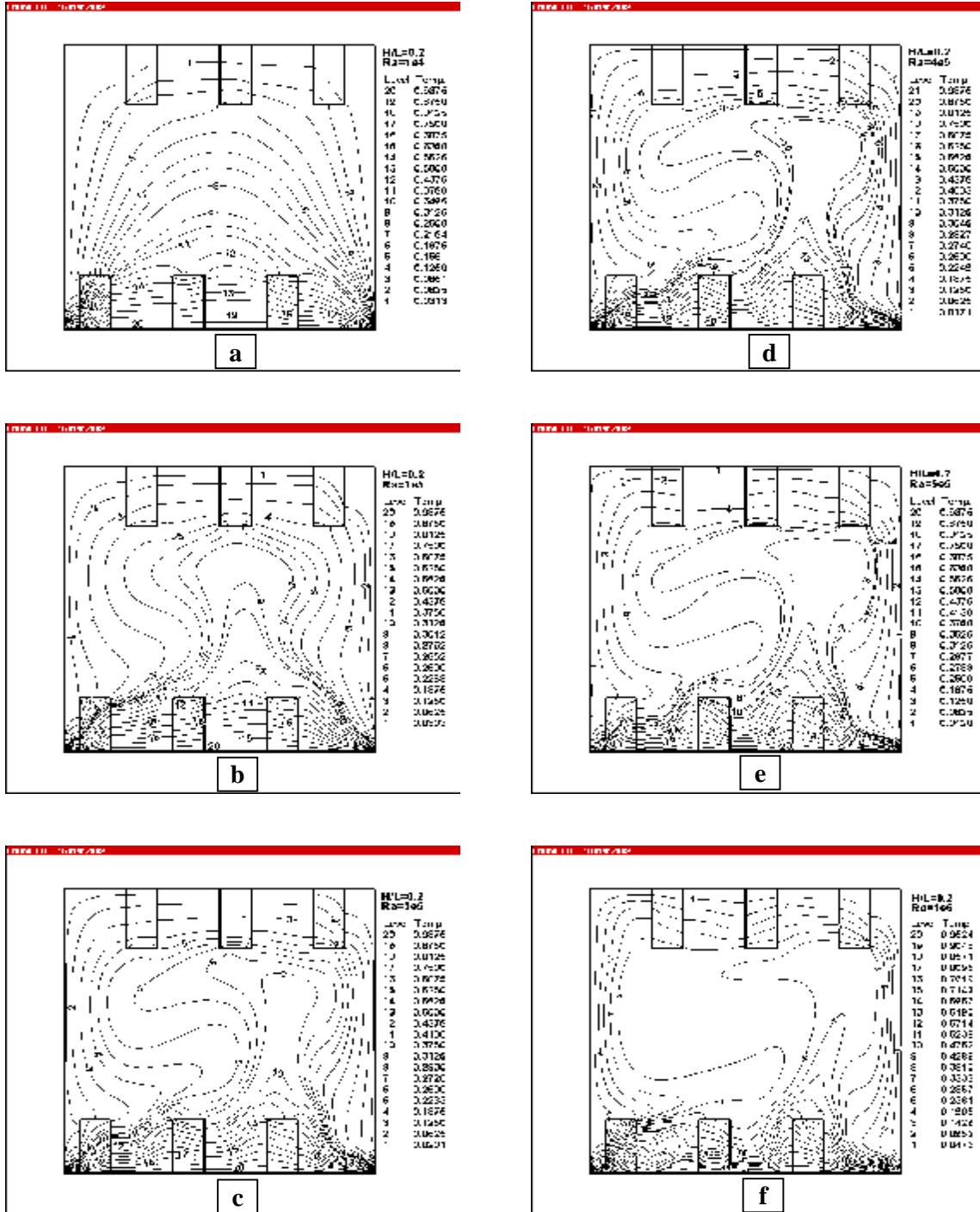


Figure (6) Temperature contours at $H/L=0.2$ with different Rayleigh Number (a. $Ra=1 \times 10^4$, b. $Ra=1 \times 10^5$, c. $Ra=3 \times 10^5$, d. $Ra=1 \times 10^4$, e. $Ra=5 \times 10^5$, and f. $Ra=1 \times 10^6$).

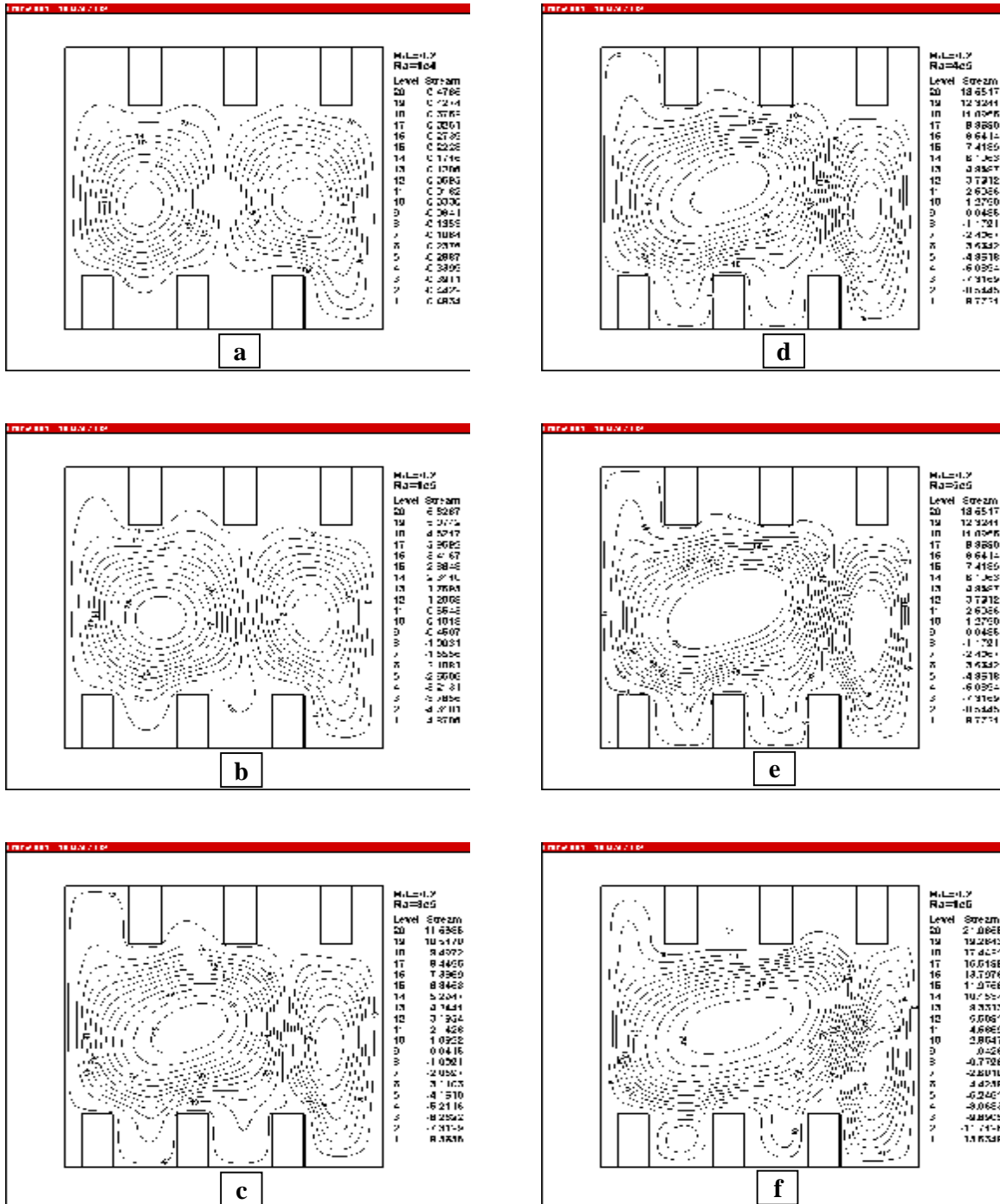


Figure (7) Stream contours at $H/L=0.2$ with different Rayleigh Number (a. $Ra=1 \times 10^4$, b. $Ra=1 \times 10^5$, c. $Ra=3 \times 10^5$, d. $Ra=1 \times 10^4$, e. $Ra=5 \times 10^5$, and f. $Ra=1 \times 10^6$).

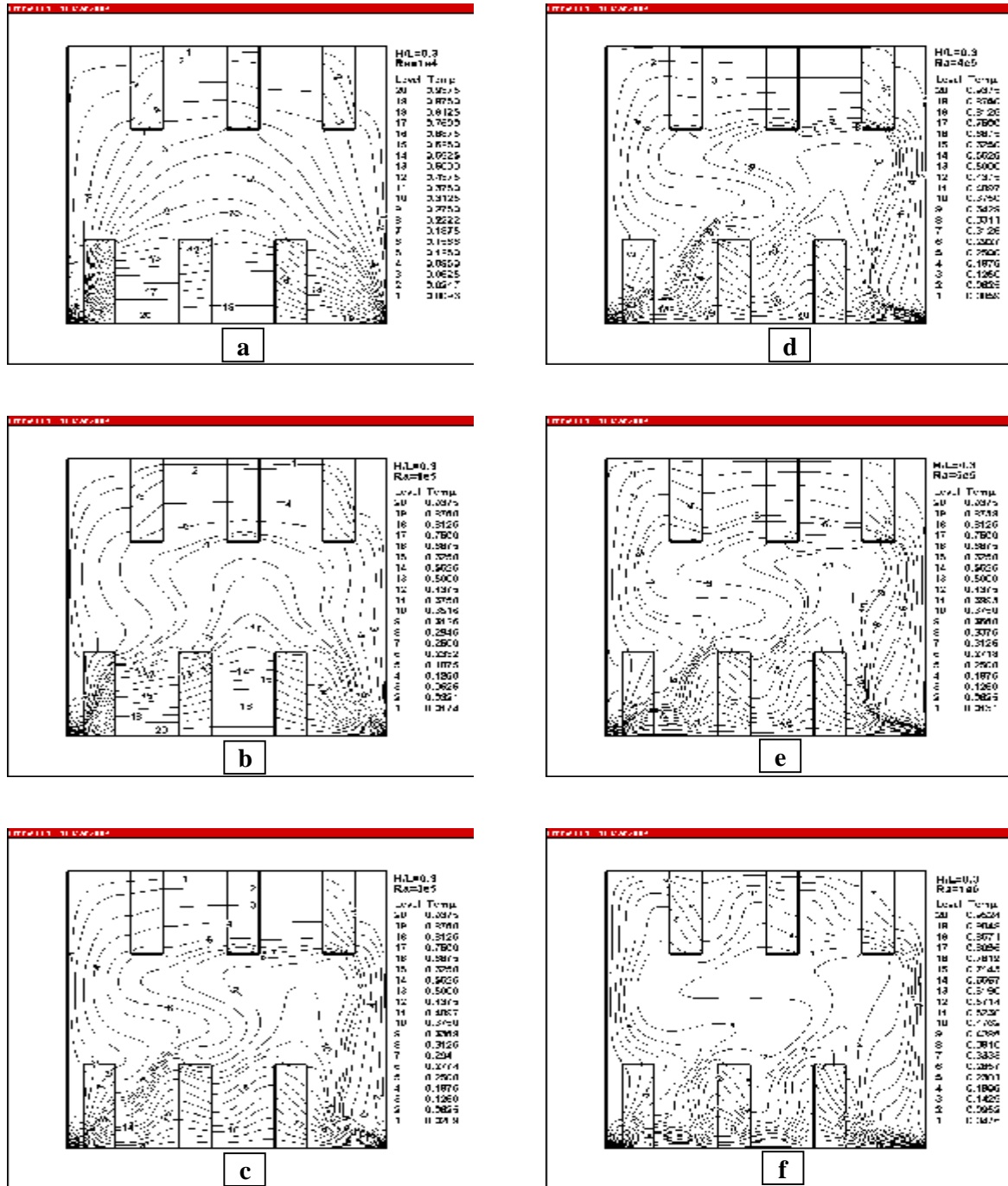


Figure (8) Temperature contours at $H/L=0.3$ with different Rayleigh Number (a. $Ra=1 \times 10^4$, b. $Ra=1 \times 10^5$, c. $Ra=3 \times 10^5$, d. $Ra=1 \times 10^4$, e. $Ra=5 \times 10^5$, and f. $Ra=1 \times 10^6$).

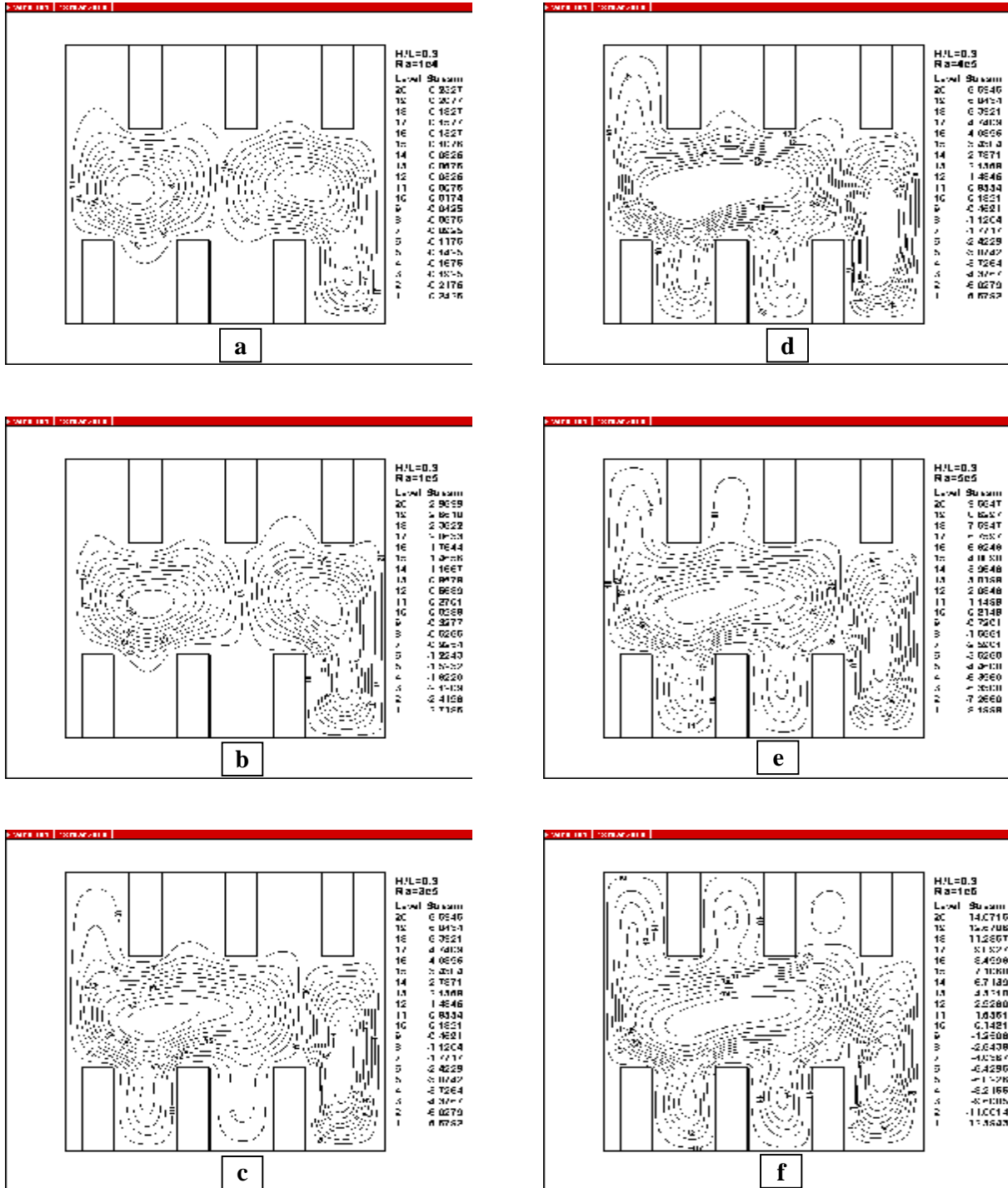


Figure (9) Stream contours at $H/L=0.3$ with different Rayleigh Number (a. $Ra=1*10^4$, b. $Ra=1*10^5$, c. $Ra=3*10^5$, d. $Ra=1*10^4$, e. $Ra=5*10^5$, and f. $Ra=1*10^6$).

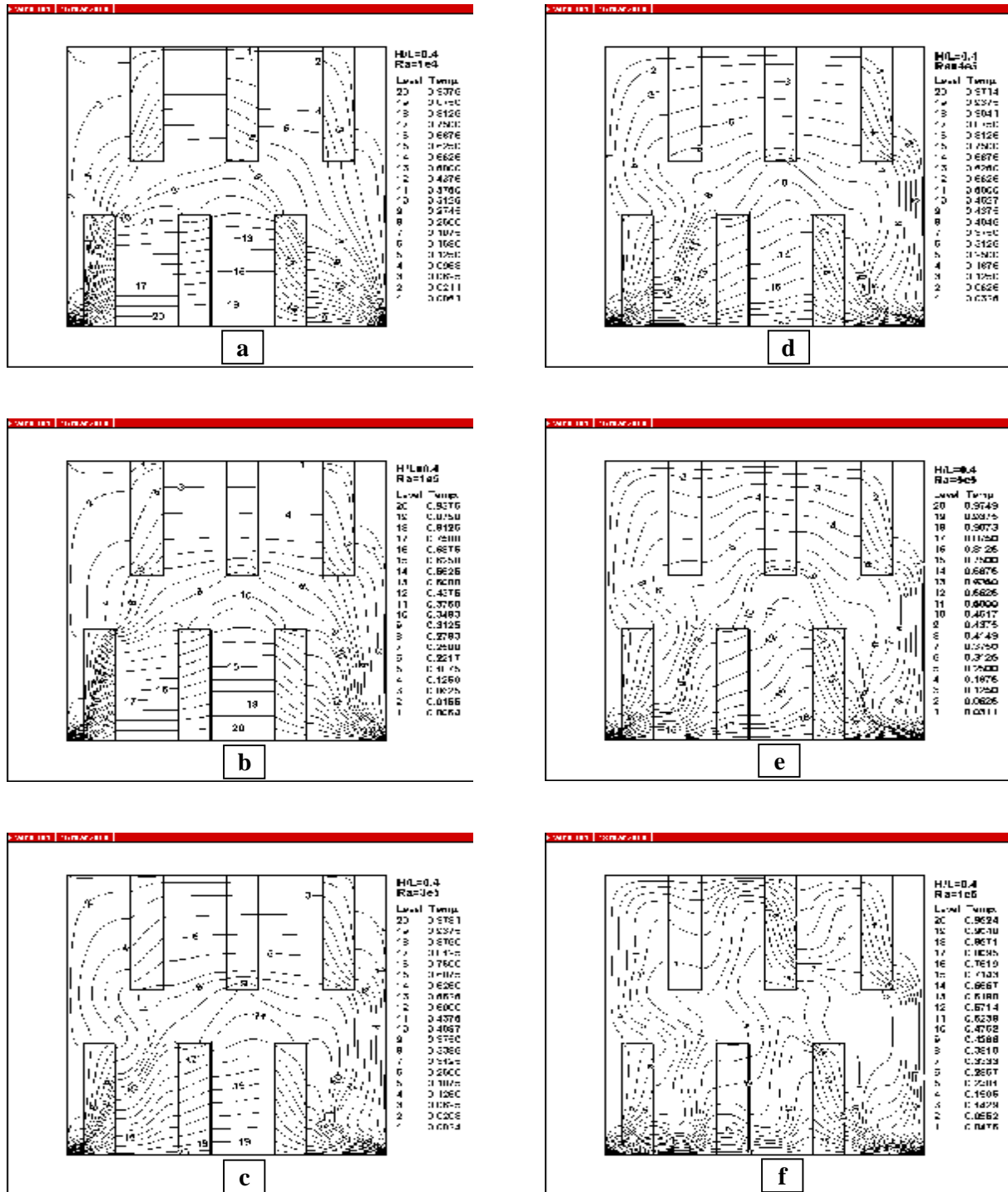


Figure (10) Temperature contours at $H/L=0.4$ with different Rayleigh Number (a. $Ra=1 \times 10^4$, b. $Ra=1 \times 10^5$, c. $Ra=3 \times 10^5$, d. $Ra=1 \times 10^4$, e. $Ra=5 \times 10^5$, and f. $Ra=1 \times 10^6$).

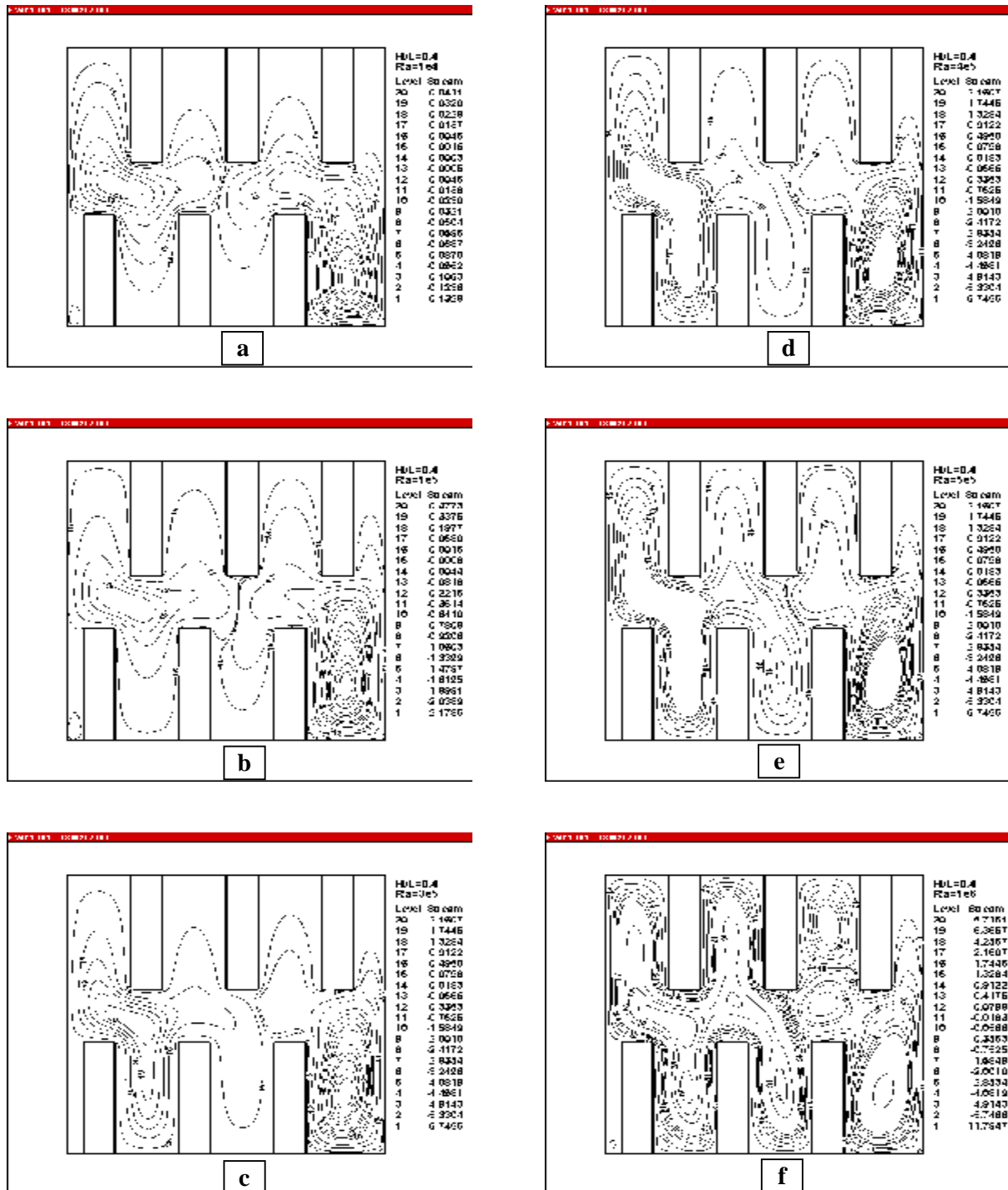


Figure (11) Stream contours at $H/L=0.4$ with different Rayleigh Number (a. $Ra=1 \times 10^4$, b. $Ra=1 \times 10^5$, c. $Ra=3 \times 10^5$, d. $Ra=1 \times 10^4$, e. $Ra=5 \times 10^5$, and f. $Ra=1 \times 10^6$).

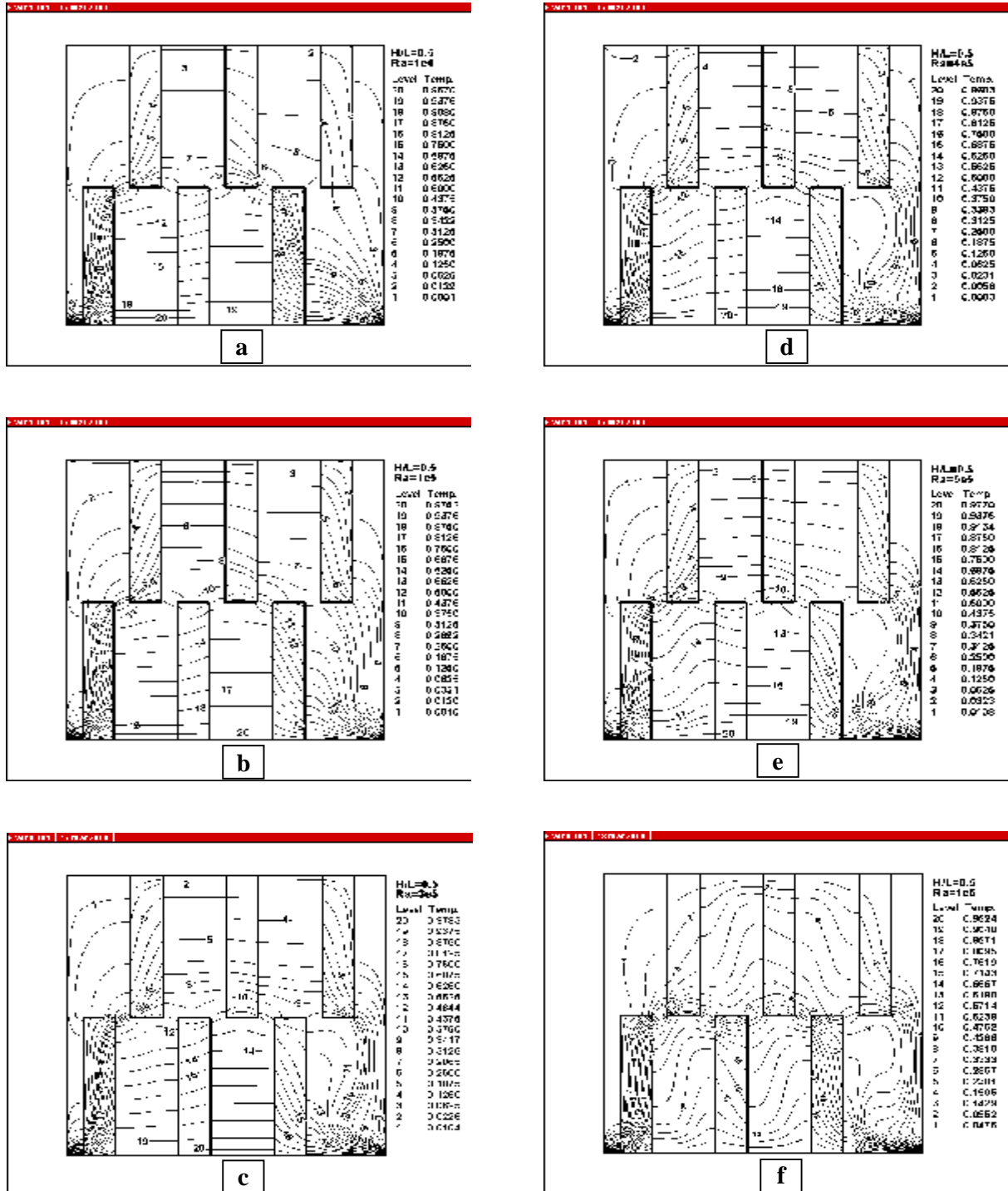


Figure (12) Temperature contours at $H/L=0.5$ with different Rayleigh Number (a. $Ra=1 \times 10^4$, b. $Ra=1 \times 10^5$, c. $Ra=3 \times 10^5$, d. $Ra=1 \times 10^4$, e. $Ra=5 \times 10^5$, and f. $Ra=1 \times 10^6$).

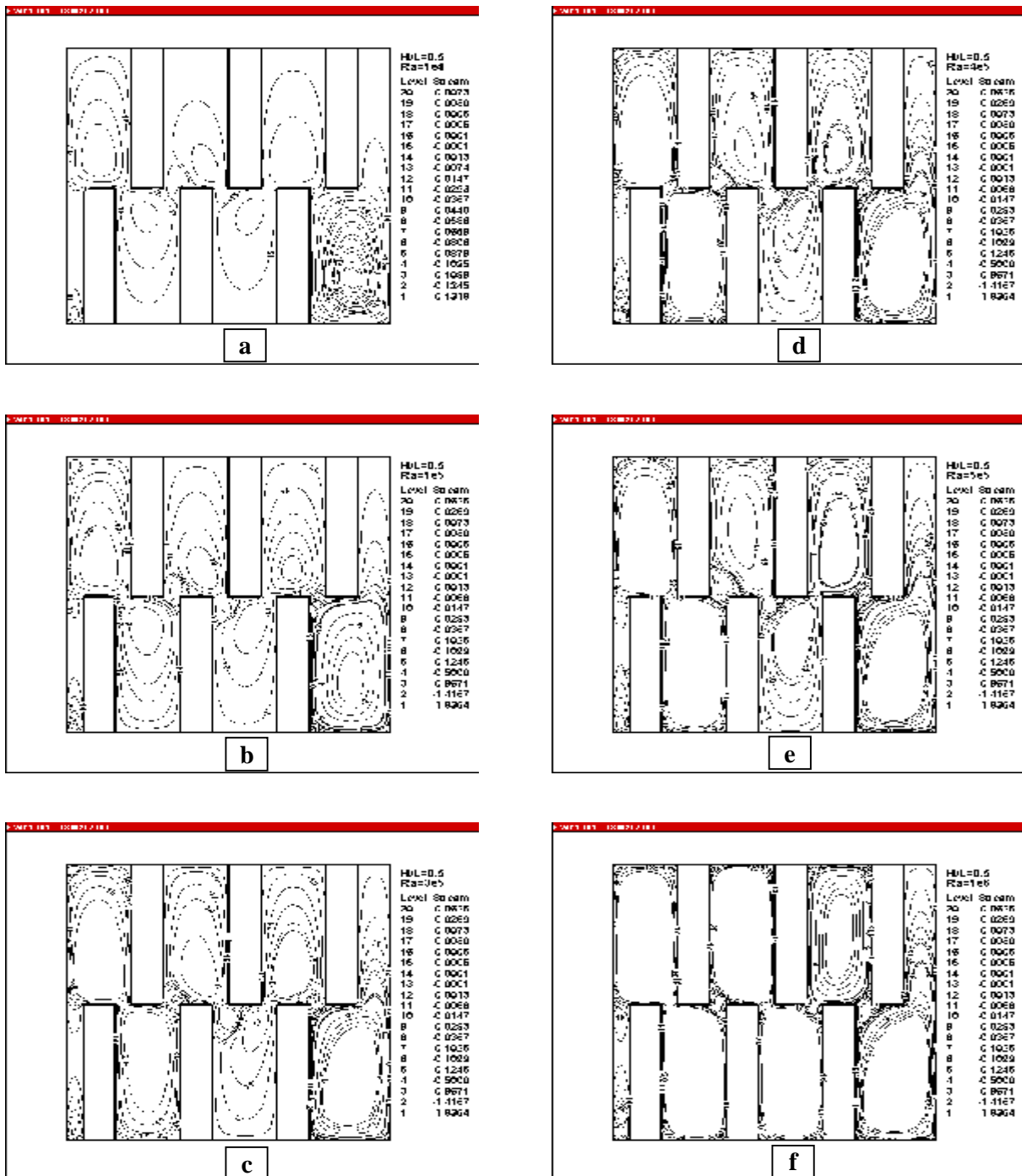


Figure (13) Stream contours at $H/L=0.5$ with different Rayleigh Number (a. $Ra=1 \times 10^4$, b. $Ra=1 \times 10^5$, c. $Ra=3 \times 10^5$, d. $Ra=1 \times 10^4$, e. $Ra=5 \times 10^5$, and f. $Ra=1 \times 10^6$).

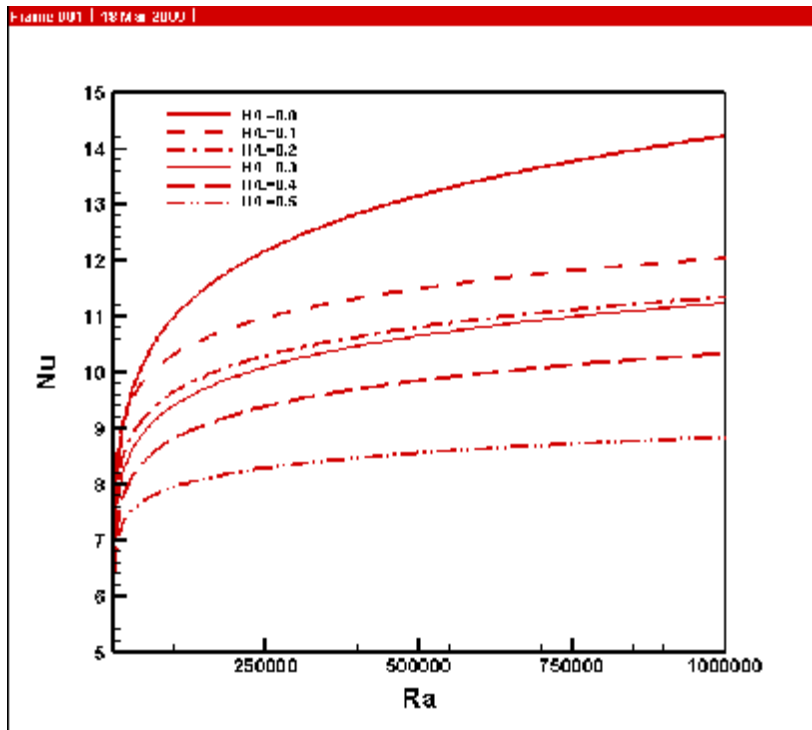
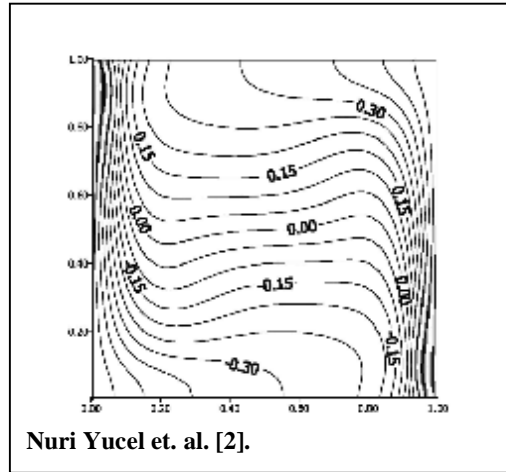
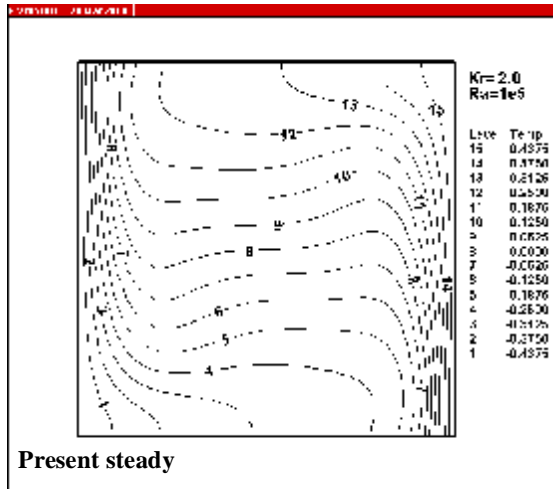
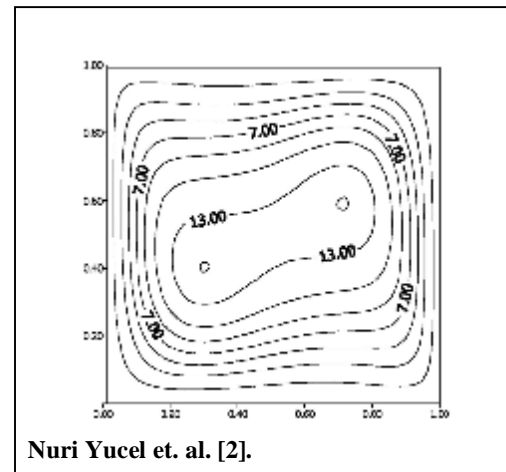
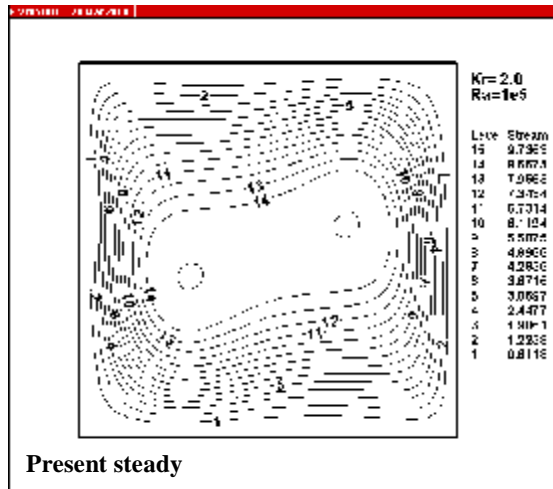


Figure (14) Variations of mean Nusselt number with the Rayleigh number at different partitions height.



a. Temperature counter comparison



a. Stream counter comparison

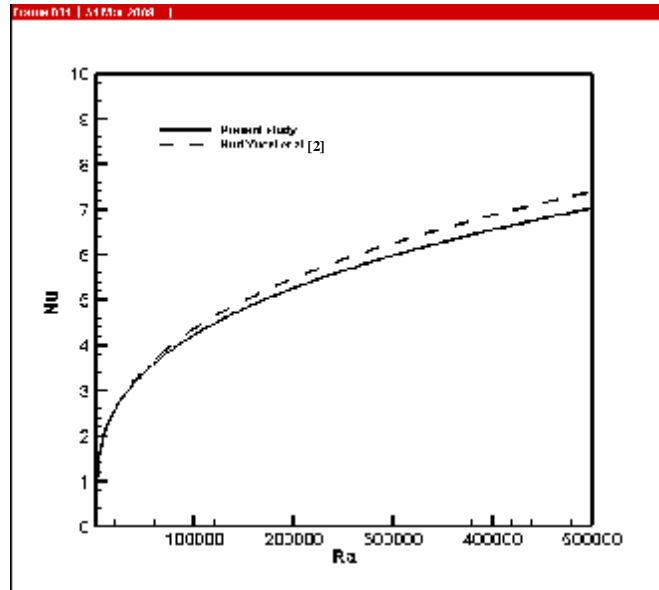


Figure (15). The comparison between the present study and ref. [2]